

**Synergistic Crystallization Regulation and Defect Passivation for Growth of
High-Quality Perovskite Single Crystals towards Ultrasensitive X-Ray Detection**

Zhilong Chen, Hu Wang, Jie Fu, Pengxiang Wang, Xin Liu, Hao Dong, Shuang Yang*, and Yuchuan Shao**

Z. L. Chen, J. Fu, P. X. Wang, X. Liu, H. Dong, Prof. H. Wang, and Prof. Y. C. Shao
Laboratory of Thin Film Optics, Shanghai Institute of Optics and Fine Mechanics,
Chinese Academy of Sciences, Shanghai 201800, P. R. China
E-mail: wanghu@siom.ac.cn and shaoyuchuan@siom.ac.cn

Z. L Chen, and Prof. S. Yang
Key Laboratory for Ultrafine Materials of Ministry of Education, Shanghai Engineering
Research Center of Hierarchical Nanomaterials, School of Materials Science and
Engineering, East China University of Science and Technology, Shanghai 200237, P.
R. China
E-mail: syang@ecust.edu.cn

P. X. Wang, X. Liu, Prof. H. Wang, and Prof. Y. C. Shao
Center of Materials Science and Optoelectronics Engineering, University of Chinese
Academy of Sciences, Beijing 100049, P. R. China

J. Fu, and H. Dong
School of Microelectronics, Shanghai University, Shanghai 201899, P. R. China

Prof. Y. C. Shao
School of Physics and Optoelectronic Engineering, Hangzhou Institute for Advanced
Study, UCAS, Hangzhou 310024, P. R. China
E-mail: shaoyuchuan@siom.ac.cn

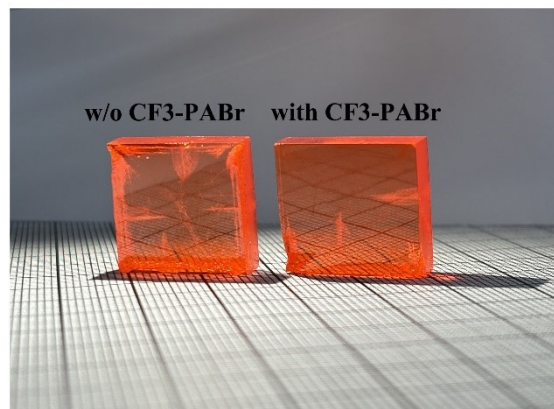


Figure S1. The photograph of MAPbBr SCs under light.

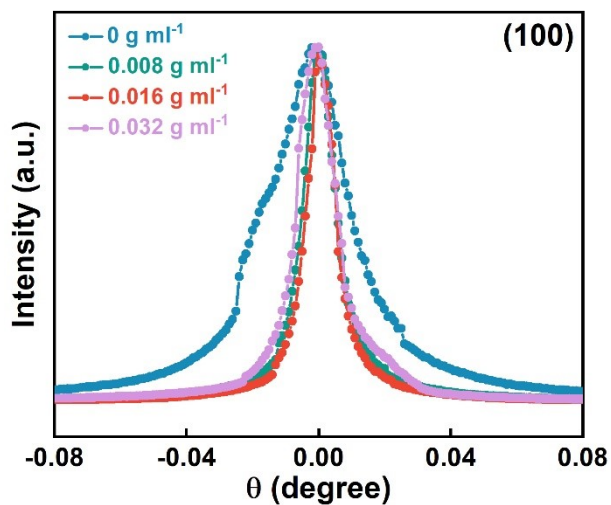


Figure S2. The XRD rocking curves of (100) plane of SCs grown with different concentrations of CF3-PABr.

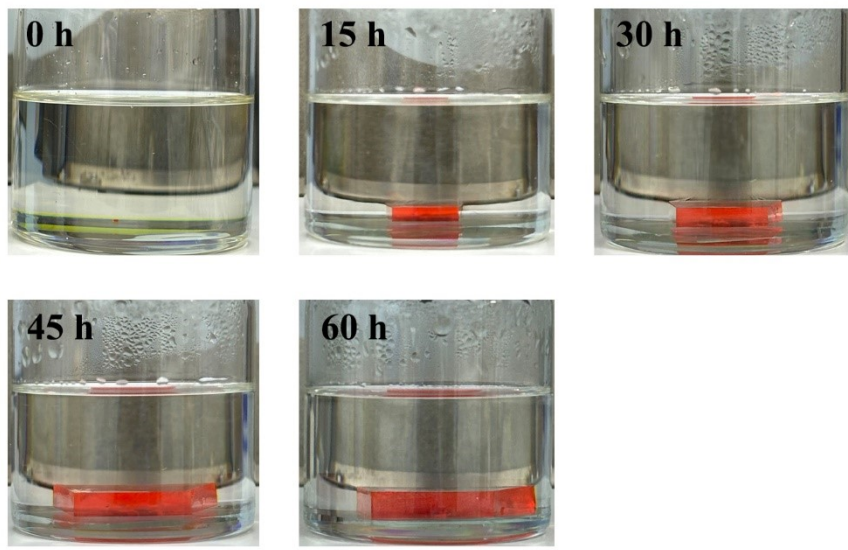


Figure S3. The photographs of growth process without CF3-PABr at a ramp rate of $0.2\text{ }^{\circ}\text{C h}^{-1}$ from $50\text{ }^{\circ}\text{C}$.

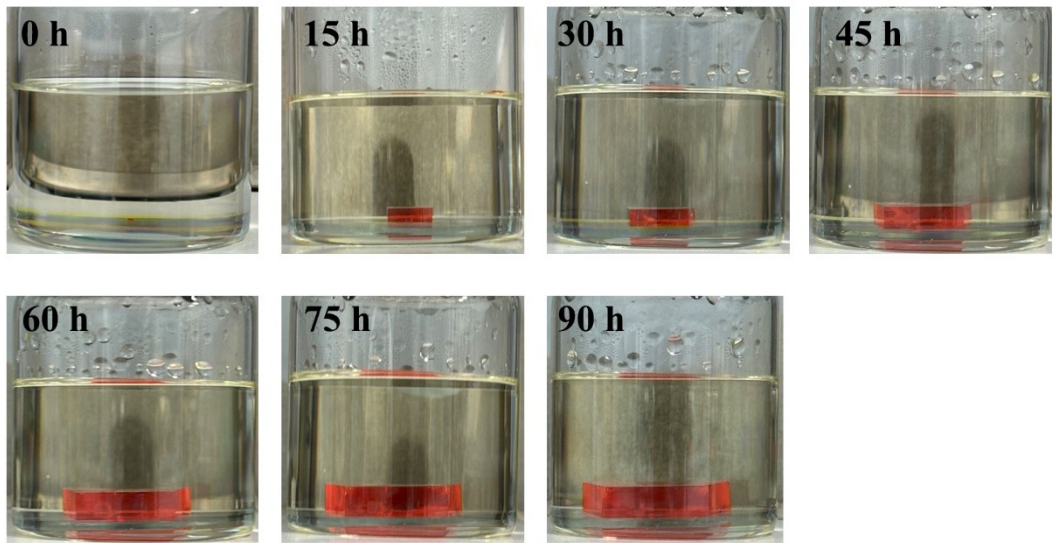


Figure S4. The photographs of growth process with CF3-PABr at a ramp rate of $0.2\text{ }^{\circ}\text{C h}^{-1}$ from $50\text{ }^{\circ}\text{C}$.

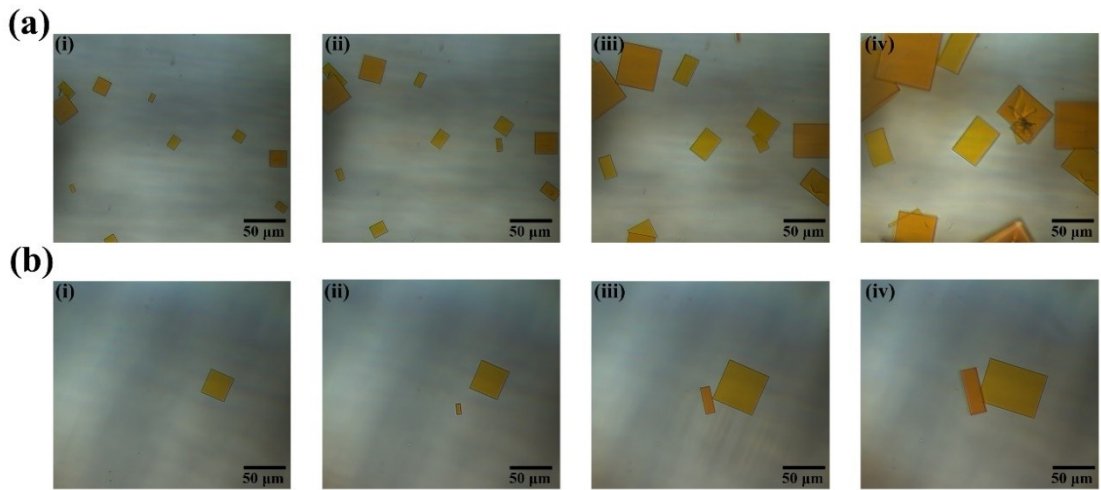


Figure S5. Optical micrographs of SCs grown from MAPbBr_3 precursor solutions (a) without and (b) with CF3-PABr at 55 °C (Recording interval is 5 mins).

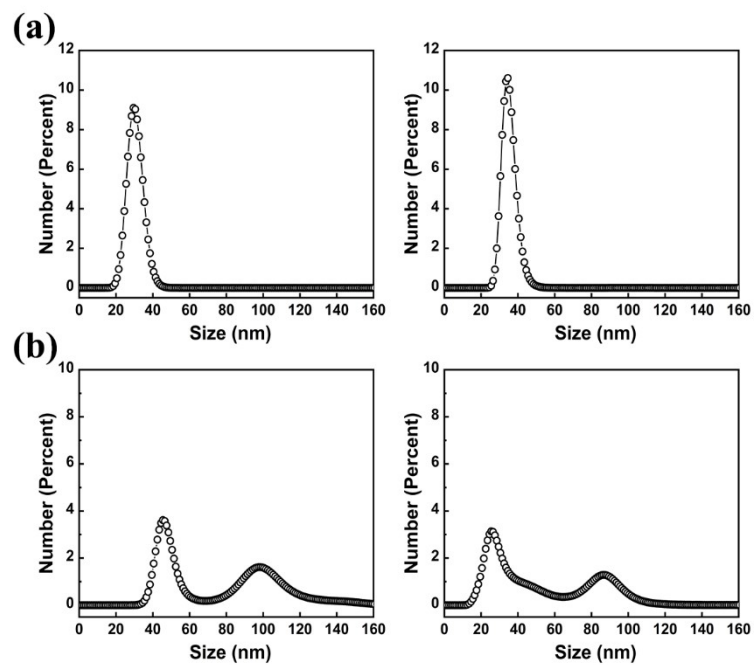


Figure S6. The repeated DLS measurements for MAPbBr_3 precursor solutions (a) without CF3-PABr and (b) with CF3-PABr.

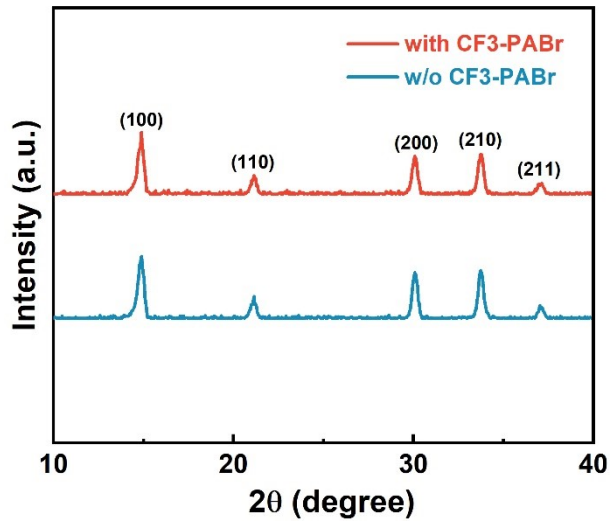


Figure S7. Powder XRD patterns of SCs grown with and without CF3-PABr.

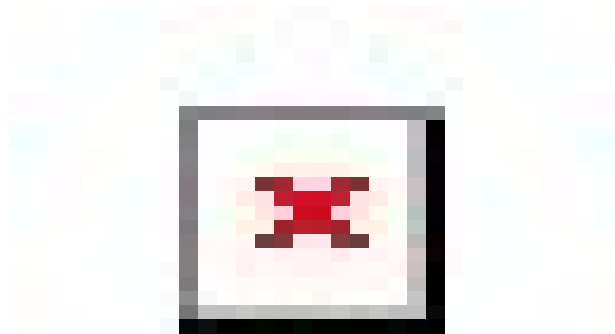


Figure S8. F 1s XPS spectra of the SC grown with CF3-PABr with different etching depths.

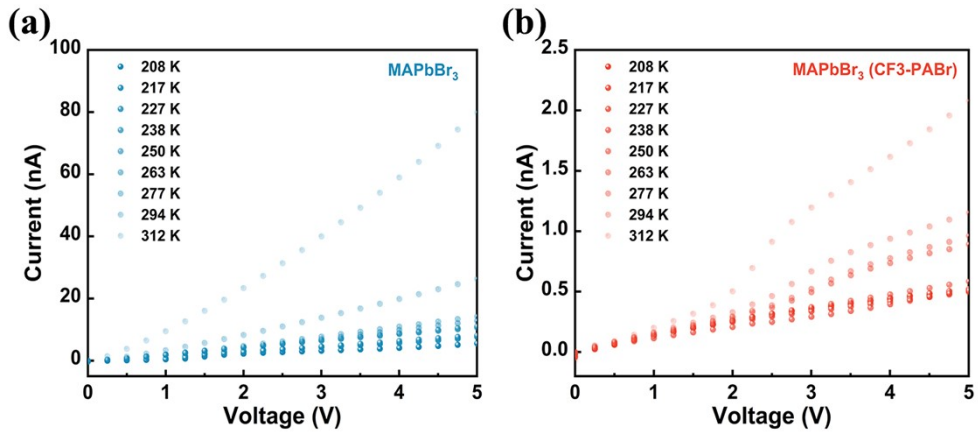


Figure S9. Current–voltage curves of Au/SC/Au devices based on SCs grown (a) without and (b) with CF3-PABr at different temperatures.

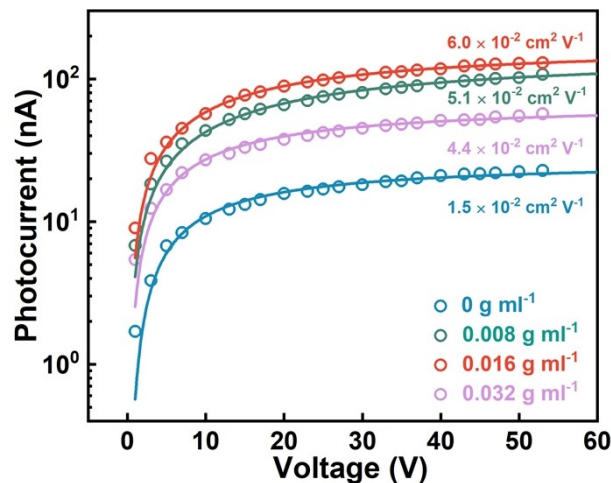


Figure S10. Photoconductivity measurements of SCs grown with different concentrations of CF3-PABr based on Au/Al/BCP/C₆₀/SC/Au devices.

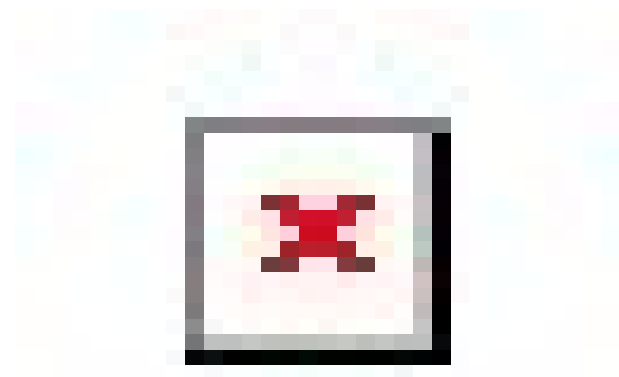


Figure S11. X-ray responses to different dose rates of the device based on the SC grown with CF3-PABr.

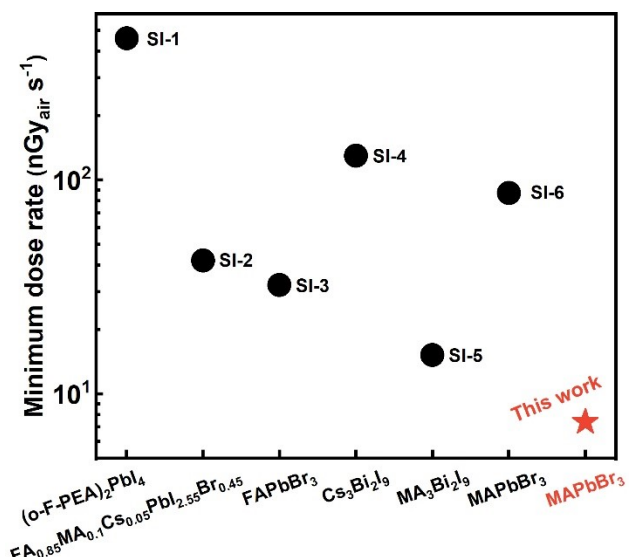


Figure S12. Summary of the minimum dose rate of the on-off responses of different X-ray detectors.

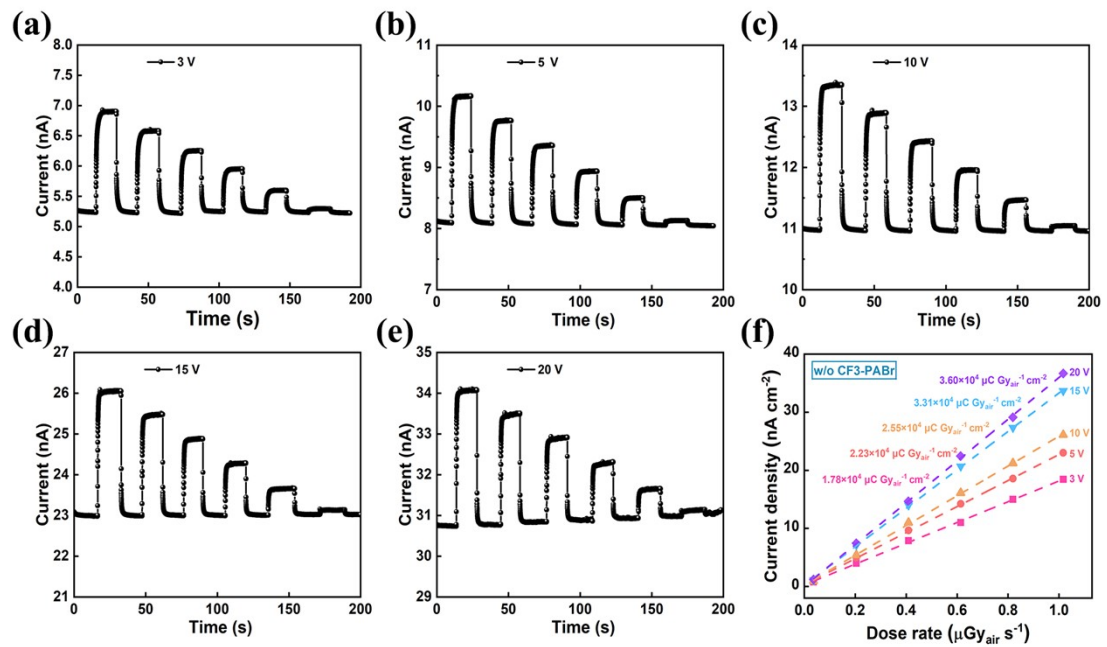


Figure S13. (a-e) X-ray responses to different dose rates and (f) the corresponding sensitivity of the device based on the SC grown without CF3-PABr.

Table S1. Summary of performance of MAPbBr₃ SC based X-ray detectors.

Year	Device structure	Sensitivity ($\mu\text{C Gy}_{\text{air}}^{-1}$ cm^{-2})	Detection limit ($\text{nGy}_{\text{air}} \text{s}^{-1}$)	Bias (V mm^{-1})	Ref
2016	Au/BCP/C ₆₀ /MAPbBr ₃ /Au	80	500	N/A	7
2017	Au/BCP/C ₆₀ /MAPbBr ₃ /Au	21000	36	46.7	8
2017	Cr/BCP/C ₆₀ /MAPbBr ₃ /Cr	84000	7.6	60	9
2018	Ag/PCBM/C ₆₀ /MAPbBr ₃ /poly- TPD/Au	23600	N/A	50	10
2019	Al/MAPbBr ₃ /Au	359	N/A	14300	11
2021	Au/MAPbBr _{2.5} Cl _{0.5} (p-i-n)/Au	36000	16	50	12
2022	Au/MAPbBr ₃ /Au	21897.44	25	25	13
2023	Au/BCP/C ₆₀ /MAPbBr ₃ /MoO _x /A u	19370	42.3	100	14
2023	ITO/MAPbBr ₃ /Au	91200	N/A	40	15
2024	Ti/MAPbBr ₃ /Au	96000	2.8	50	16
2024	Au/Al/BCP/C ₆₀ /MAPbBr ₃ /Au	108800	1.3	30	This work

Table S2. The relationship of the tube current and X-ray dose rate with two pieces of aluminum sheets for attenuation.

Tube current (μA)	Dose rate ($\mu\text{Gy}_{\text{air}} \text{s}^{-1}$)
133	1.017
106.4	0.819
79.8	0.614
53.2	0.409
26.6	0.204
5	0.036

Table S3. The relationship of the tube current and X-ray dose rate with three pieces of aluminum sheets for attenuation.

Tube current (μA)	Dose rate ($\text{nGy}_{\text{air}} \text{s}^{-1}$)
26.6	41
13.3	20
5	7.4

References

1. B. B. Zhang, Z. Xu, C. Ma, H. J. Li, Y. C. Liu, L. L. Gao, J. Zhang, J. X. You and S. Z. Liu, *Adv. Funct. Mater.*, 2021, **32**, 2110392.
2. Y. C. Liu, Y. X. Zhang, X. J. Zhu, J. S. Feng, I. Spanopoulos, W. J. Ke, Y. H. He, X. D. Ren, Z. Yang, F. W. Xiao, K. Zhao, M. Kanatzidis and S. Z. Liu, *Adv. Mater.*, 2021, **33**, 2006010.
3. W. Jiang, J. W. Ren, H. B. Li, D. Liu, L. J. Yang, Y. Xiong and Y. Y. Zhao, *Small Methods*, 2023, **7**, 2201636.
4. Y. X. Zhang, Y. C. Liu, Z. Xu, H. C. Ye, Z. Yang, J. X. You, M. Liu, Y. H. He, M. G. Kanatzidis and S. Z. Liu, *Nat. Commun.*, 2020, **11**, 2304
5. S. J. Tie, W. Zhao, D. Y. Xin, M. Zhang, J. D. Long, Q. Chen, X. J. Zheng, J. G. Zhu and W. H. Zhang, *Adv. Mater.*, 2020, **32**, 2001981.
6. L. R. Chen, H. Wang, W. Q. Zhang, F. H. Li, Z. Y. Wang, X. Y. Wang, Y. C. Shao and J. D. Shao, *ACS Appl. Mater. Interfaces*, 2022, **14**, 10917-10926.
7. H. T. Wei, Y. J. Fang, P. Mulligan, W. Chuirazzi, H. H. Fang, C. Wang, B. R. Ecker, Y. L. Gao, M. A. Loi, L. Cao and J. S. Huang, *Nat. Photonics*, 2016, **10**, 333-339.
8. W. Wei, Y. Zhang, Q. Xu, H. T. Wei, Y. J. Fang, Q. Wang, Y. H. Deng, T. Li, A. Gruverman, L. Cao and J. S. Huang, *Nat. Photonics*, 2017, **11**, 315-321.
9. H. T. Wei, D. DeSantis, W. Wei, Y. H. Deng, D. Y. Guo, T. J. Savenije, L. Cao and J. S. Huang, *Nat. Mater.*, 2017, **16**, 826-833.
10. X. Wang, D. W. Zhao, Y. P. Qiu, Y. Huang, Y. Wu, G. W. Li, Q. Q. Huang, Q. Khan, A. Nathan, W. Lei and J. Chen, *Phys. status solidi*, 2018, **12**, 1800380.
11. Q. Xu, W. Y. Shao, Y. Li, X. L. Zhang, X. Ouyang, J. Liu, B. Liu, Z. Y. Wu, X. P. OuYang, X. B. Tang and W. B. Jia, *ACS Appl. Mater. Interfaces*, 2019, **11**, 9679-9684.
12. X. Wang, Y. Xu, Y. Pan, Y. Li, J. Xu, J. Chen, J. Wu, Q. Li, X. Zhang, Z. Zhao, C. Li, E. E. Elemike, D. C. Onwudiwe, J. Akram and W. Lei, *Nano Energy*, 2021, **89**, 106311.
13. W. Q. Zhang, H. Wang, H. Dong, F. H. Li, Z. Y. Wang and Y. C. Shao, *J. Mater. Chem. C*, 2022, **10**, 17353-17363.
14. M. Y. Han, Y. R. Xiao, C. Zhou, Z. J. Xiao, W. Y. Tan, G. W. Yao, X. X. Wu, R. Z. Zhuang, S. M. Deng, Q. Hu, Y. X. Yang, Z. H. Tang, X. S. Zhou, H. B. Lin, H. L. Liang, S. H. Lin, Z. X. Mei, C. L. Wang, Q. Chen, W. Zhang and Y. Jiang, *Adv. Funct. Mater.*, 2023, **33**, 2303376.
15. M. K. Kim, Y. S. Choi, D. Kim, K. Heo, S. J. Oh, S. Lee, J. An, H. Yoo, S. H. Kim, T. S. Kim and B. Shin, *ACS Appl. Mater. Interfaces*, 2023, **15**, 57404-57414.
16. W. Q. Zhang, H. Wang, Z. L. Chen, P. X. Wang, X. Liu, H. Dong, J. L. Zhao, Y. Cui and Y. C. Shao, *ACS Appl. Mater. Interfaces*, 2024, **16**, 12844-12852.

